Robust Multi-Look HRR ATR Investigation through Decision-Level Fusion Evaluation

Bart Kahler
General Dynamics
WPAFB, OH 45433

Erik Blasch
Air Force Research Lab
WPAFB, OH 45433

Abstract *– Simultaneous Tracking and identification (STID) is impacted by sensor and target dynamics especially in move-stop-move type scenarios. For most scenarios, both moving and stationary targets can be processed into 1-D High-Range Resolution (HRR) Radar profiles which contain enough feature information to discern one target from another to help maintain track or to identify the vehicle. To meet mission objectives, different decision-level and feature-level classifiers can be designed to achieve performance requirements such as the sensitivity of the number of features for a given location accuracy, identification confidence, timeliness (revisit rate and track length), and throughput of the number of targets tracked. For robust STID evaluation, repeatable scenarios, metrics, and data support is recommended for comparisons. This paper compares the ATR performance of a baseline single-look algorithm to the performance of decision level and feature level fusion ATR algorithms through multilook assessments to assess relative fusion performance gains.*

Keywords: *ATR, Information Fusion, HRR, eigen-value, SVD, Fusion Evaluation*

1 Introduction

For robust simultaneous tracking and identification (STID) [1, 2] the determination of target type, dynamics, and intent is important. Radar is all-weather and distant invariant, eliminating the need for classifier changes over environmental conditions.[3] For this reason, many surveillance systems incorporate High Range Resolution (HRR) radar and synthetic aperture radar (SAR) modes to be able to capture moving and stationary targets. Feature-, signature-, and categorical-aided tracking and automatic target recognition (ATR) applications have benefited from HRR radar modes. Determining the quality of information can assist in joint tracking and ID [4] or joint tracking and classification [5, 6] through analysis by Bayes, Dempster-Shafer, or DSmT methods [7].

For robust STID methods, intelligent sensor management optimizes over the parameters. In search mode, it would be desirable to stay far way to find targets (track initiation).[8, 9] As targets are acquired, the tracker operates in a track maintenance mode to follow targets; however, to maintain track when the targets are closely spaced such as at road intersections requires feature analysis to identify the targets. HRR radar provides the dynamic processing analysis for both detection for tracking and signal features (range, angle, aspect, and peak amplitudes) for automatic target recognition (ATR).

ATR consists of assessing the data, designing a classifier based on trained data, comparing the trained data to measured data through a classifier, and testing the results. Typically, ATR, or information fusion object assessment, developers tailor their algorithms to a specific data set. Having designed the initial algorithm, they have a point solution. Further studies and analysis are required to robustly determine the capability of different classifiers, performance of classifiers over different operating conditions, and the sensitivities and bounds of performance. To enable the further analysis, developers should consider developing a Challenge Problem Set (CPS). A CPS affording information fusion evaluation includes real and synthetic data, baseline algorithms, truth data for sensitivity analysis, defined metrics, and stated experiments or challenges.

Some notable data sets include the Tracking Benchmark problem [10], the Moving and Stationary Automatic Target Recognition (MSTAR) data set [11] that provides SAR collections, and the ImageFusion.org site that contains electro-optical (EO) and Infrared (IR) data. [12, 13] To complement these methods, and further explore STID, there is a need for HRR data sets. Compiling a HRR data set would enable robust explorations in information fusion object assessment over multi-look position and feature algorithm analysis and comparisons.

Multi-look classifier development typically includes training on the location and peak features of a 1-D HRR signature. [14] Classifiers have been developed for correlation [15], Bayes and Dempster Shafer information fusion approaches [16], entropy and Information theory analysis [17], and Neuro-Fuzzy methods [18]. The classifier results have been used for tracking [19] and multi-look HRR[20]. Other approaches include eigen-value template matching [21], Eigen-extended maximum average correlation (EEMACH) filters [22] and likelihood methods accounting for Rician, Amplitude, specular, and diffuse, Cisoid scattering[23] .

The eigen-template matching offers a robust approach to ATR because of the ability to determine the log-likelihood analysis in consideration of the robust nature of the system. Eigen-templates have been used for 2D ATR problems using Electro-optical [24], SAR, [25, 26], and Forward-looking IR (FLIR) analysis [27, 28]. In each of these methods, the Eigen-template matching provides a

Report Documentation Page

Form Approved
OMB No. 0704-0188

1. REPORT DATE	2. REPORT TYPE	3. DATES COVERED
JUL 2008		**00-00-2008 to 00-00-2008**

4. TITLE AND SUBTITLE	5a. CONTRACT NUMBER
Robust Multi-Look HRR ATR Investigation through Decision-Level Fusion Evaluation	5b. GRANT NUMBER
	5c. PROGRAM ELEMENT NUMBER
6. AUTHOR(S)	5d. PROJECT NUMBER
	5e. TASK NUMBER
	5f. WORK UNIT NUMBER
7. PERFORMING ORGANIZATION NAME(S) AND ADDRESS(ES) **Air Force Research Laboratory,Wright Patterson AFB,OH,45433**	8. PERFORMING ORGANIZATION REPORT NUMBER
9. SPONSORING/MONITORING AGENCY NAME(S) AND ADDRESS(ES)	10. SPONSOR/MONITOR'S ACRONYM(S)
	11. SPONSOR/MONITOR'S REPORT NUMBER(S)

12. DISTRIBUTION/AVAILABILITY STATEMENT
Approved for public release; distribution unlimited

13. SUPPLEMENTARY NOTES
11th International Conference on Information Fusion, June 30 ? July 3, 2008, Cologne, Germany

14. ABSTRACT
see report

15. SUBJECT TERMS

16. SECURITY CLASSIFICATION OF:			17. LIMITATION OF ABSTRACT	18. NUMBER OF PAGES	19a. NAME OF RESPONSIBLE PERSON
a. REPORT	b. ABSTRACT	c. THIS PAGE			
unclassified	**unclassified**	**unclassified**	**Same as Report (SAR)**	**8**	

stable analysis for a single look. The eigenvector approach was then adapted and refined by Shaw [29, 30, 31] and others [23] for 1-D template formation using HRR profile data. To increase robustness, we seek to develop a multi-look approach utilizing the eigen-template feature analysis [32], summarized by a classifier confusion-matrix and combine them for enhanced HRR target identification.

This paper develops a multi-look identification for HRR using decision and feature-level fusion approaches with the Baseline Automated Recognition of Targets (BART) technique to distinguish between multiple moving targets in clutter. Section 2 discusses the motivation, purpose, and problem methodology. Section 3 introduces the HRR identification methodology using the eigen-template approach. Section 4 discusses the fusion of the classifiers. Section 5 presents results and Section 6 draws conclusions.

2 HRR Data Processing

Focused one dimensional HRR profiles of moving targets may be generated with enhanced target-to-clutter ratios via Doppler filtering or other methods. One such procedure first chips the moving target from the motion compensated video phase history data and aligns the target chips for clutter suppression and focusing. This results in a two dimensional range-Doppler chip that is masked using binary morphology to determine the mean clutter level, target length, and target edges in the chip. The range-Doppler chip is then cropped about the Doppler extent of the target mask before computing the mean of all sub-aperture images. The maximum scatters from each range bin are kept to form the 1-D HRR profile.

Stationary targets from SAR imagery may also be formed into 1-D HRR profiles using a similar process. For targets in SAR imagery, constant-false alarm rate (CFAR) detection is performed first, followed by target mask formation using binary morphology. The formation process crops around the target mask and computes the mean of all sub-aperture images, keeping the maximum scatters from each range bin to form the stationary HRR profile. Shown in **Figure 1** is the general profile formation process flow.

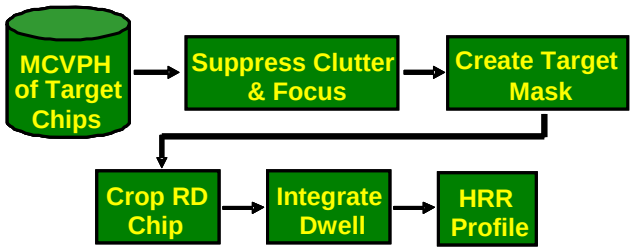

Figure 1. 1-D HRR Profile formation Process

Recent research [33] has shown that HRR profiles formed from SAR imagery of stationary targets have comparable features to profiles of the same moving target at corresponding collection geometries as shown in **Figure 2**.

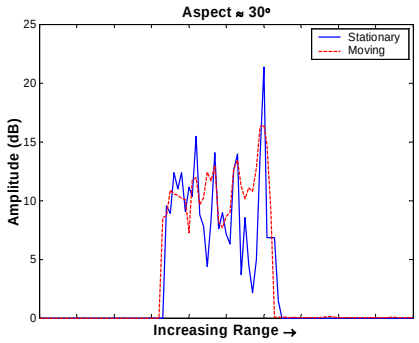

Figure 2. Comparison of moving / stationary 1-D HRR profiles

3 Baseline ATR Algorithm

Pattern recognition algorithms applied to Automatic target recognition (ATR) problems are typically trained on a group of desired objects in a library to gain a statistical representation of each objects' features. The algorithm then aligns input signatures to the library templates (or models [34]) and determines the best correlation value for the aligned features. Algorithms often apply a threshold to the best score to reject questionable objects before identification or class label decisions are made. Although this process seems straight forward, misidentification or rejection of an input object as a viable target occurs because of conditions such as the target being obscured from the sensor, target adjacent to another object, and target transition from moving to stationary and back to a moving state in a traffic scenario, that unexpectedly alters the features used in the identification process.

The stationary target signatures of the public Moving and Stationary TArget Recognition (MSTAR) data set have been extensively studied and creatively applied to the synthetic aperture radar (SAR) ATR problem. A number of techniques have been explored by Novak[25-26] and others in the development of 2-D SAR image classification algorithms which utilized the MSTAR data. The importance and impact of extended operating conditions to ATR performance were assessed in a number of papers using this data set [17,35,36]. The MSTAR data was even processed into 1-D HRR profiles to evaluate potential HRR ATR solutions [1, 37, 38, 39].

The Baseline Automated Recognition of Targets (BART) algorithm is based on the eigen template techniques described extensively in the literature. In principal, templates are formed from the dominant eigenvector and the algorithm is trained on features found in the HRR profile data, leading to the creation of a library. The vehicle features of the templates in the library are then compared to the features found in the test signatures, ultimately resulting in an ATR decision.

3.1 Template Formation

The Power Transform operation defined as, $\mathbf{Y} = \mathbf{X}^{v}$ was used to map non-Gaussian HRR data to have Gaussian-like density. In [21] it had been demonstrated that application of power transform on noiseless detected HRR data tended to enhance HRR performance considerably. However, the BART algorithm used in this work does not apply the power transform operation because HRR data collected under real world conditions can be potentially noisy causing the power transform to enhance clutter in the HRR profile as well as the target energy. The noise amplification can be mitigated by preprocessing the HRR profiles and clipping any clutter present (noiseless) before applying the power transform. But, the BART algorithm was designed to use the HRR profiles without any knowledge of what preprocessing was or was not applied to the data prior to the algorithm. The Singular Value Decomposition (SVD) operation used in template formation projects the information contained in the detected HRR profile matrix onto orthogonal basis spaces, known as Karhunen-Loeve Transformation or Principal Component Analysis.

The HRR profile training data is first sorted in azimuth and then organized into a range-angle map. The training data is then windowed in aspect to the desired template coverage size. For the templates formed to produce the results presented in this paper, a training data window of 5° in aspect and 1° in depression was used because of the generally sparse nature of the HRR data set and to avoid outliers potentially biasing templates. A statistical representation of the block of training data is determined by using SVD to decompose the normalized range-angle maps of HRR profiles for each template into orthogonal basis spaces. The three resulting matrices from the decomposition can be written as shown in Eq. 1 below where the range and angle subspaces are decoupled into left and right eigenvectors.

$$\boldsymbol{X} = \mathbf{U}\,\boldsymbol{\Sigma}\,\mathbf{V}^{T} \qquad (1)$$

In Eq. 1 the range-angle map, **X**, is an $l \times m$ sized matrix written as the product of the orthogonal basis spaces where the $l \times l$ sized left singular vector, **U**, contains the range subspace. $\boldsymbol{\Sigma}$ is an $l \times m$ sized diagonal matrix of nonzero decreasing singular values. The $m \times m$ sized right singular vector, **V,** contains the angle subspace which is discarded in the template formation process. The first singular value in $\boldsymbol{\Sigma}$ is the largest eigen value and corresponds to the first range-space eigenvector in **U** shown by Shaw [21,29-31] to contain a significant portion of the range profile feature energy. The dominant range-space eigenvectors are used as matching templates in the BART algorithm.

These templates were stored at a reported average template azimuth for each window of data used. For example all of the training data between 0° and 5° was used to form the template at 2.5°, and the training data between 5.01° and 10° was used to form the template at 7.5°. The process is repeated until all templates are formed for each object in the library.

3.2 Threshold Formation

Following template formation the threshold statistics are determined by first normalizing the training data. The training data is then centroid aligned to the features in the templates. The centroid aligning is accomplished for each HRR profile by circularly shifting an integer number of range bins to the left (negative shift). The *correlation score* for the shifted profile to that of the template is computed. Then shift the profile one range bin to the right and recompute the correlation score, keeping the maximum correlation and optimal range bin shift value. The process is repeated for all ± integer range bin shifts. A typical integer shift value of ±10 is a good starting point. Once the optimal shifts are found for all of the training data in a template window, the mean and standard deviation of the maximum correlations are computed for the template. The process of testing the training HRR profile data against its own template is repeated for each template formed earlier. The results are used to compute a *threshold* for target rejection which is represented by

$$\mathbf{T} = \bar{\boldsymbol{x}} + \boldsymbol{f} * \boldsymbol{s} \qquad (2)$$

Where **T** is the rejection threshold, $\bar{\boldsymbol{x}}$ is the mean of the maximum correlations for a given template aspect window, **s** is the standard deviation of the maximum correlations of a given template window, and **f** is the scale factor which adjusts the operating point along the receiver operator curve (ROC). A target rejection threshold is computed for each library object and every template aspect angle using Eq. 2. The results presented later in this paper are for a factor, **f** = 0.5.

3.3 Decision Process

At this point, the training process of the BART algorithm is complete with the creation of a vehicle library containing training statistics and templates that may then be used in the identification of ground vehicles. Target recognition begins with the normalization of the test signature followed by choosing the template closest in azimuth to the estimated test profile aspect angle. The test data is then centroid aligned to the features of the chosen template. This is achieved by circularly shifting an integer number of test profile range bins to the left and computing the correlation score for the shifted profile to that of the template. Then the test data is shifted a range bin to the right and the correlation score is determined again. After shifting through all ± integer range bin shifts, the maximum score is kept for the test profile and selected template. The process is then repeated using the same vehicle profile with every object in the library, resulting in a vector of best scores. Now the maximum score in the vector is found and the corresponding library threshold is computed. The threshold is applied by comparing the

maximum score to the threshold with scores less than the threshold being labeled an *unknown* and all other scores resulting in the test profile being labeled as the library object corresponding to the selected threshold. The process is repeated for all test signatures and the results are tracked so that a decision ATR *confusion matrix* can be compiled as shown in the results (Sect. 5).

3.4 Metric Presentation

The Baseline Automated Recognition of Targets (BART) algorithm of the HRR ATR Challenge Problem Set utilized the eigen-value HRR approach as a baseline method, although other methods could be incorporated. The likelihood vectors were compiled into a confusion matrix (CM). Thus, each single look provided a full analysis of the classifier, *C*, for all target comparisons. The likelihood vectors of the confusion matrix allowed for a more thorough analysis with such performance criteria as detection and false alarm probabilities, respectively P_D and P_{FA}. The confusion matrix lists a sets of likelihood values with the real targets as the rows $\{T_1, \ldots, T_N\}$, and the testable hypothesis as the columns $\{T_1, \ldots, T_N, \text{other}\}$,

$$CM = \begin{bmatrix} & T_1 & \ldots & T_N & \text{other} \\ T_1 & \ldots & & \vdots & \\ & \ldots & & \vdots & \\ T_N & & & \ldots & \vdots \end{bmatrix} \quad (3)$$

Representing the likelihood values in the confusion matrix as:

$$CM = \begin{bmatrix} A & B & \ldots & B & O \\ C & D & \ldots & D & O \\ \vdots & \vdots & \ldots & \vdots & \vdots \\ C & D & \ldots & D & O \end{bmatrix} \quad (4)$$

From the confusion matrix, and a defined target-to-confusion ratio as *m*, a set of metrics can be identified to support analysis including:

$$P_{\text{Declaration}} = \frac{A}{A + B} \quad (5)$$

$$P_{\text{FalseAlarm}} = \frac{C}{C + D} \quad (6)$$

$$P_{\text{Correct Classification}} = \frac{m \bullet P_D}{(m \bullet P_D) + P_{FA}} \quad (7)$$

4 Multi-Look ID Fusion

The ability to perform track and identity fusion requires sensor-processed classifications from different levels. Multi-target data association algorithms that accurately track targets in the presence of clutter assume that the detected targets can be tracked from a sequence of center-of-gravity and pose positional data. Detected classification can effectively discern the target for a given scenario using experience of target movement, training, or predicted information. For example, identifying a target requires the correct orientation and speed estimate. Two targets of the same type may be crossing in space, but since they can not occupy the same location, they would each have a different orientation relative to a sensor. By exploiting the orientation, velocity, and multi-resolution feature information, each target can be assessed for the correct track-ID association.

The capability of a sensor to track and identify targets simultaneously includes finding the target center for tracking, determining the target pose, and searching the neighboring characteristics for discerning salient features for association to a specific target type. By partitioning kinematic and target feature data, associations at different levels can be used for either coarse(tracking) or fine (recognition) target analysis. For example, features [40] can be used to identify targets with a level of uncertainty; however, if many features are fused, the identity improves and helps eliminate clutter. The tracker must use the available features to discern an object (*identify* a target) which is a subset of Automatic Target Recognition (ATR). Certain features are inherently more useful in recognizing a target than others. For instance, identifying a large car versus a small car would result from an analysis of the length-to-width ratio but, obtaining these features is a function of sensor resolution. Additionally, decoupling information can be used for a single-platform observer to fuse information from a sequence of sensor data or for a multiple-platform scenario in which fusing is performed from different geometrical positions. Further information on the development of the STID derivation is found in [1].

The problem of track level and ID-level fusion has characteristic *tradeoffs* about which the tracker must decide. For close targets, it is useful to keep an accurate track on multiple targets. The intelligent processor performs target-to-ID association at multiple levels and can either track targets at a low resolution or ID targets at a higher resolution. By leveraging knowledge about target features, fusion algorithms can significantly reduce processing time for tracking and identifying targets. For separated targets, resources may exist to identify each target. Hence, due to a limited set of resources and/or processor time, a trade-off exists between the identification and tracking of a target which is coupled to the classifier.

In the case of multiple ATR systems observing the same area, the HRR profiles can be at significantly different geometries meaning that the features associated with a target will differ for each ATR. In such a case a decision-level fusion approach is good solution since the ATR decisions are fused and not the features of the target signatures. If however; a single sensor is observing a target over time, the HRR profiles will be closely associated in aspect and the target features can be fused from multiple looks (feature-level fusion) for an enhanced profile that may then be used for track maintenance or target ID. By leveraging knowledge about target types, fusion algorithms can significantly reduce processing time for tracking and identifying targets.

4.1 Decision Level Fusion (DLF) Method

The decisions from an ATR are often stored in a confusion matrix which is an estimate of likelihoods. For the single-look ATR performance these estimates are treated as priors. The decision level fusion technique presented here uses the decision c_{1j} from ATR-1 as a priori performance estimate and the decisions from multiple ATRs or multiple geometries for a single ATR $c_{2k,}\, c_{3k,}\, c_{4k}$, … c_{nk} to declare T_i the target if it is determined to be the most reliable decision.

A single target ID is declared by fusing all previous looks with the current *n*-look to obtain an optimal result. The DLF technique estimates the probability

$$P(T_i \mid c_{1j}, c_{2k,}\, c_{3k,}\, c_{4k}, \ldots c_{nk}), \qquad \forall\ i, j, \text{ and } k. \tag{8}$$

where c_{1j} indicates that ATR-1 declares target *j*, c_{2k} is the declaration of target *k* by ATR-2, c_{3k} means ATR-3 called target *k*, and c_{nk} means ATR *n* made target call *k*. The probability that target *i* is present given n declarations have occurred is given by $P(T_i \mid c_{1j}, c_{2k,}\, c_{3k,}\, c_{4k}, \ldots c_{nk})$. Eq. 8 can be written using Bayes' Theorem as

$$P(T_i \mid c_{1j}, c_{2k,}\, c_{3k,}\, c_{4k}, \ldots c_{nk}) \tag{9}$$
$$= \frac{P(c_{1j}, c_{2k}, c_{3k}, c_{4k}, \ldots c_{nk} \mid T_i) P(T_i)}{\sum_i P(c_{1j}, c_{2k}, c_{3k}, c_{4k}, \ldots c_{nk} \mid T_i) P(T_i)}$$

for all *i*, *j*, *k*, and *n* decisions. Eq. 9 can be simplified assuming that the prior probabilities $P(T_i)$ are all equal to

$$P(T_i \mid c_{1j}, c_{2k}, c_{3k}, c_{4k}, \ldots c_{nk}) = \tag{10}$$
$$\frac{P(c_{1j}, c_{2k}, c_{3k}, c_{4k}, \ldots c_{nk} \mid T_i)}{\sum_i P(c_{1j}, c_{2k}, c_{3k}, c_{4k}, \ldots c_{nk} \mid T_i)}$$

for all *i*, *j*, *k*, and *n* decisions. Assuming that ATR 1 through ATR n provide independent identification declarations, the joint probabilities in Eq. 10 can be factored to

$$P(T_i \mid c_{1j}, c_{2k}, c_{3k}, c_{4k}, \ldots c_{nk}) = \tag{11}$$
$$\frac{P(c_{1j} \mid T_i) P(c_{2k} \mid T_i) P(c_{3k} \mid T_i) P(c_{4k} \mid T_i) \ldots P(c_{nk} \mid T_i)}{\sum_i P(c_{1j} \mid T_i) P(c_{2k} \mid T_i) P(c_{3k} \mid T_i) P(c_{4k} \mid T_i) \ldots P(c_{nk} \mid T_i)}$$

for all *i*, *j*, *k*, and *n* decisions. Now the right side of Eq. 11 is in terms of the entries of the ATR-1 confusion matrix and each index of the matrix represents a probability of identification for the given target (rows) versus the declared target (column). Let $d(j, k)$ represent the fusion algorithm declaration given that ATR-1 declares target *j* and ATR-2 through ATR-n declares target *k* where $d(j, k) = T_m$, where $m = max\{P(T_i \mid c_{1j}, c_{2k,}\, c_{3k,}\, c_{4k}, \ldots c_{nk})\}$. The highest probability is declared the target after computing the probability of target *i* for all target declarations.

Assuming independence, the decision level fusion [41] performance is predicted by estimating, for each target of interest T_i, the frequency with which the ATR 1 algorithm makes the declarations *j* and *k*, and assigning from Eq. 11 the appropriate declaration T_m. The frequency that T_j is declared can be computed for each T_i resulting in a performance estimate for the decision level fusion algorithm in the form of a confusion matrix [42].

$$P(c_{1j}, c_{2k,}\, c_{3k,}\, c_{4k}, \ldots c_{nk} \mid T_i) \tag{12}$$
$$= P(c_{1j} \mid T_i)\, P(c_{2k} \mid T_i)\, P(c_{3k} \mid T_i) \ldots P(c_{nk} \mid T_i)$$

for all *i*, *j*, *k*, and *n* looks.

For a large number of looks, the cumulative approach becomes computationally intense and although an optimal decision will result, the computational burden is excessive and timely decisions unlikely. Therefore, the technique is simplified to use the decisions from two ATR's with the resulting fused output being treated as a prior and sequentially incorporating each new ATR decision.

For example, if only two ATR's decisions c_{1j} indicating ATR-1 declared target *j* and c_{2k} indicating that ATR-2 declared target *k* are used, Eq. 11 reduces to

$$P(T_i \mid c_{1j}, c_{2k}) = \frac{P(c_{1j} \mid T_i) P(c_{2k} \mid T_i)}{\sum_i P(c_{1j} \mid T_i) P(c_{2k} \mid T_i)} \tag{13}$$

for all *i*, *j*, and *k*.

Determining the highest probability the fusion algorithm makes a target declaration d. The fused result replaces the ATR-1 decision, c_{1j} in Eq. 13. Another ATR decision represented by c_{3k} replaces ATR 2, giving

$$P(T_i \mid d_{1j}, c_{3k}) = \frac{P(d_{1j} \mid T_i) P(c_{3k} \mid T_i)}{\sum_i P(d_{1j} \mid T_i) P(c_{3k} \mid T_i)} \tag{14}$$

for all *i*, *j*, and *k*.

Once again the highest probability is determined and a sequentially fused declaration is made, d_{2j}. This process is iteratively applied for each additional ATR decision and in general can be written as

$$P(T_i \mid d_{oj}, c_{nk}) = \frac{P(d_{oj} \mid T_i) P(c_{nk} \mid T_i)}{\sum_i P(d_{oj} \mid T_i) P(c_{nk} \mid T_i)} \tag{15}$$

for all *i*, *j*, and *k*. Where d_{oj} represents the o^{th} fused decision declaring target *j* and c_{nk} is ATR n declaring target *k*. This technique reduces the decision level fusion implementation to an operation between two confusion matrices regardless of the number of looks involved.

4.2 Feature Level Fusion (FLF) Method

As discussed previously, the baseline ATR algorithm (BART) employs an Eigen-template formation method via SVD. For a 1–D HRR profile, the template formation process combines the features from a range-angle map of training data covering for example 5 degrees in azimuth. A logical extension of this technique is to adapt it for 1-D profile feature fusion for multi-look identification of moving ground vehicles. In tracking and ID applications a series of looks at a target that are closely associated in aspect can have the features of the signatures fused

together to reduce noise and the influence of outliers in any single profile. The fusion process for 1-D HRR profiles would closely emulate the template formation process presented in the literature by forming a range-angle map of *n*-looks at a target and performing an SVD operation on the data to obtain the dominant eigenvector that has been shown [21,29-31] to contain the majority of the target energy. The eigen vector (EV) method has been shown to work for normalized HRR profiles with and without a power transform and the approach used for template formation is reproduced below but for multi-look 1-D HRR profiles at closely associated aspect angles with the goal to produce a fused multi-look test profile.

First, 1-D HRR profiles are sorted by estimated azimuth from *n*-looks to create a range-angle map, $\mathbf{X} \in \Re^{m \times n}$, of *m* range bins by *n* aspect angles. This matrix is decomposed via SVD into three corresponding orthogonal basis spaces shown in Eq 16.

$$\mathbf{X} \xrightarrow{\text{SVD}} \mathbf{U}\,\mathbf{\Lambda}\,\mathbf{V}^{\mathrm{T}} = \sum_{i=1}^{n} \lambda_i \mathbf{u}_i \mathbf{v}_i^{\mathrm{T}} \tag{16}$$

where the range space contains the left eigen vectors to be used as features in the multi-look ID process are represented by

- **Range-Space**:

$$\mathbf{U} = EV[\mathbf{X}\mathbf{X}^{\mathrm{T}}] = [\mathbf{u}_1, \ldots, \mathbf{u}_m] \in \Re^{m} \tag{17}$$

which is the expected value of range sequences. The angle space or right eigen vectors are discard in this process but are represented as

- **Angle-Space**:

$$\mathbf{V} = EV[\mathbf{X}^{\mathrm{T}}\mathbf{X}] = [\mathbf{v}_1, \ldots, \mathbf{v}_n] \in \Re^{n} \tag{18}$$

and the singular values are given by

- **Singular Values :**

$$\mathbf{\Lambda} = Diag[\lambda_{11}, \ldots, \lambda_{nn}] \in \Re^{n} \tag{19}$$

Where, EV[…] represents the operation "Eigen-Vectors of" **U** an **V** in Eq 17 and Eq 18. For Range Vs. Angle HRR data, the range and angle sub-spaces are decoupled via SVD into the left eigen vectors (**U**) that span the orthogonal basis space in the range domain while the right eigen vectors (**V**) span the angle space. **Λ** is diagonal containing *n* ($m > n$ is assumed here) singular values in decreasing order, $\lambda_{11} \geq \lambda_{22} \geq \ldots \geq \lambda_{nn}$, where λ_{ii} denotes the weights associated with i-th eigenvector and λ_{11} is the largest singular value and implies a significant amount of profile energy contributed to the particular eigen-vector. Hence these are denoted as "signal subspace" eigenvectors whereas those corresponding to the smaller singular values are denoted as "noise or clutter subspace". The primary goal of this work is to exploit the information contained in the decoupled range basis space vectors in **U** to perform the effective ATR. The fused multi-look HRR profile is contained in u_1 of Eq 17.

The Log-likelihood of the Eigen method is given by

$$L(f_k \mid T_i) = -\frac{1}{2}\mathrm{Log}(N_0) - \sum_{n=1}^{N} \frac{[\bar{f}_k(n) - \mu_{ik}(n)]^2}{N_0} \tag{20}$$

$$\text{where} \quad \bar{f}_k(n) = f_k(n) / \sum_{n=1}^{N} f_k(n) \tag{21}$$

The amplitude-location features $f_k(n)$ are estimated through the SVD approach where the HRR test profiles matrix $\mathbf{X}_i$ are formed by the column vectors of x_d that correspond to the features

$$\mathbf{X}_i = [x_d]_{d \in T_t} \xrightarrow{\text{SVD}} \mathbf{U}\,\mathbf{\Lambda}\,\mathbf{V}^{\mathrm{T}} \tag{22}$$

where $\{f_k(n)\} = \{u_1(n)\}$ and $f_k(n)$ is found as the left singular vector of $\mathbf{X}_i$ corresponding to the greatest singular value.

5 Results

The results presented in this section used measured data processed into 1-D HRR profiles from a scenario where ten ground vehicles were traveling in the open along a roadway under benign conditions. Single look performance of the BART algorithm was generated from all available data to gage relative improvement gains using the fusion techniques described earlier. The DLF technique was used with five confusion matrices each produced with a unique sample set from the HRR data base by the BART algorithm. The eigenvector feature level multi-look fusion technique was use to generate a database of test profiles for a 5-look scenario. The results of these experiments are presented in the sections that follow.

5.1 BART Single-Look Performance

To generate the single look baseline ATR performance ten trials were generated, leaving out one of the targets in the

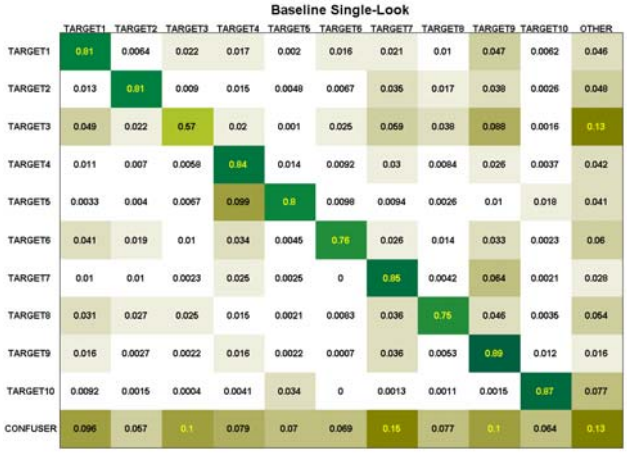

Figure 3. Single-Look Performance

library for each test, commonly called the Leave-One-Out-Method (LOOM). The results of all ten trials were combined to produce the average performance for all targets and an out-of-library confusing target shown in **Figure 3**.

For the most part the single look performance is very reasonable with the lone exception being target 3 in the confusion matrix. The distribution of the out-of-library target was uniformly confused across the entire BART algorithm library indicating that no bias toward a library object was present.

5.2 DLF Multi-look Performance

To create the DLF performance in the confusion matrix shown in **Figure 4** below, the HRR profile test data was divided by sorting the data in azimuth and taking every fifth sample to create 5 unique data sets. For each data set ten trials were run with one of the library targets removed to simulate a confusing target. The data from all ten trials was combined to create an average performance confusion matrix for each unique data set (look), five in all.

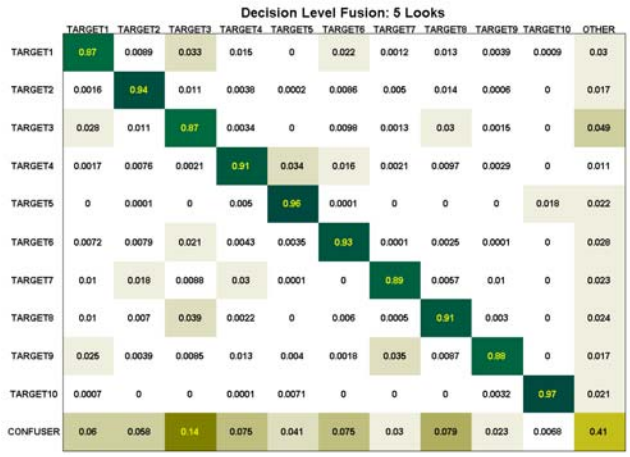

Figure 4. Decision Level Fusion Performance: 5 Looks

The DLF algorithm was first run on looks one and two with the remaining looks being added sequentially and the fused decision from the previous run being treated as prior knowledge of the targets of interest.

A significant performance gain is observed from these trials with target 3 achieving very high identification performance with respect to the baseline results. The off diagonal target confusion was significantly reduced relative to the other methods (Baseline and FLF).

5.3 FLF Multi-look Performance

The results presented in **Figure 5** are of five consecutive looks at a target fused into a single profile. The FLF profile was then tested against the BART library. Ten trials were conducted where a target in the library was removed for each trial and treated as a confuser like in the single-look performance tests. The results from all trials were combined to create the average performance for all in-library and out-of-library targets.

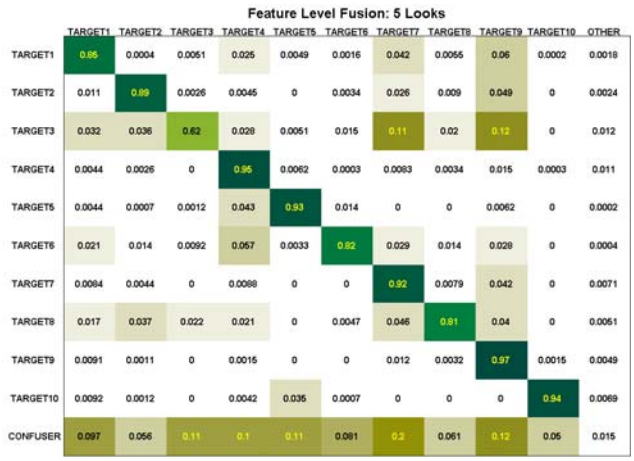

Figure 5. Feature Level Fusion Performance: 5 Looks

Although still the poorest performing target, Target 3 identification performance has improved using the FLF technique over the single look baseline results.

Finally, a set of metric comparisons, as defined in Section 3, are shown in **Figure 6**, where the first bar is the single-look case and the second bar is the multi-look case, presented over the ten target types. From this example, not every case of multi-look improves individual target recognition, but in general there is improvement.

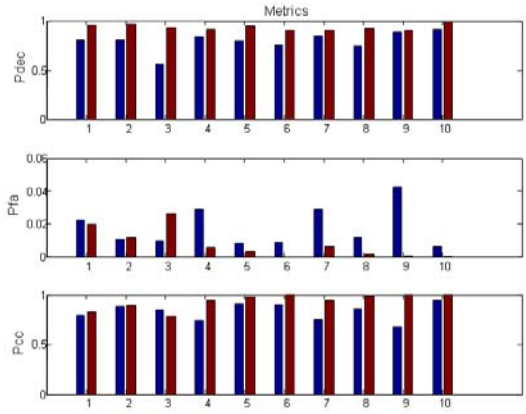

Figure 6. Multi-Look to Single-Look Comparisons.

6 Discussion & Conclusions

Both multi-look fusion techniques improved target identification performance in comparison to the baseline single-look ATR results. The five look performance of the FLF algorithm more closely resembled the baseline results. The DLF algorithm performed extremely well for the data set under test showing significant performance gains over both the baseline and feature level fusion algorithms. Evidence of the robust nature of the DLF approach can be found in the enhanced identification performance of Target 3 where both the baseline and FLF methods demonstrated similar but much lower target recognition probability caused by algorithm sensitivities to the greater percentage of extended operating conditions

present in the Target 3 data relative to the other nine targets in the data set.

Conventional measurement tracking techniques have difficulty with data association when position measurements are close. To further assess simultaneous tracking and ID algorithms, it is important to have a defined Challenge Problem set for comparison. We have presented the BART approach utilizing the Eigen ATR method provided a confusion matrix. While experiments are on-going to improve the HRR performance model robustness, some defined challenges (for sensitivity analysis) include (1) determining the performance over aspects, a set of window aspects, and aspect diversity, (2) varying the class size and mix of target types, (3) compare fusion methods and classifier approaches and mixes of both, and (4) developing different collection geometries to be included in a dynamic sensor manager utilization. Together, these experiments will lead to a robust understanding of fusion performance evaluation and the methodology can be extended to other data sets.

7 References

[1] E. Blasch, *Derivation of A Belief Filter for High Range Resolution Radar Simultaneous Target Tracking and Identification*, Ph.D. Diss., Wright State University, 1999.

[2] E Blasch and C. Yang, "Ten methods to Fuse GMTI and HRRR Measurements for Joint Tracking and ID", *Fusion 04*, July 2004.

[3] W. Snyder and G. Ettinger, "Performance Models for Hypothesis-Level Fusion of Multi-Look SAR ATR", *Proc. SPIE* 2003.

[4] J. Lancaster, S. Blackman, "Joint IMM/MHT Tracking and Identification for MultiSensor Ground Tracking, Fusion06, 2006.

[5] S. Mori, C-Y. Chong, E. Tse, and E. P. Wishner, "Tracking and Classifying Multiple Targets Without A Priori Identification," *IEEE Trans. On Automatic Control*, Vol AC-31, No. 5, May 1986.

[6] D. Angelova & L. Mihaylova, "Joint Tracking and Classification with Particle Filtering and Mixture Kalman Filtering using Kinematic Radar Information," *Digital Signal Processing*, 2005.

[7] A. Tchamova, J. Dezert, et al, "Target Tracking with Generalized data association based on the general DSm rule of combination," *Fusion04*, 2004.

[8] Y. Bar-Shalom & X. Li, *Multitarget-Multisensor Tracking: Principles and Techniques*, YBS, New York, 1995.

[9] S. Blackman and R. Popoli, *Design and Analysis of Modern Tracking Systems*, Artech House Publisher, Boston, 1999.

[10] T. Kirubarajan, Y. Bar-Shalom, W. D. Blair, and G. A. Watson, "IMMPDAF for Radar Management and Tracking Benchmark with ECM," *IEEE Trans. Aero. & Elect. Sys.*, Vol 34, No. 4, Oct 1998.

[11] T.D. Ross, J.J. Bradley, L.J. Hudson, M.P. O'Connor, "SAR ATR – So What's the Problem? – An MSTAR Perspective", *Proc. of SPIE*, Vol. 3721, 1999.

[12] S. Hudson, and Psaltis, D., "Correlation Filters for aircraft identification from radar range profiles", *IEEE Trans. AES*, 1993.

[13] Visible & Infrared TNO images from www.imagefusion.org.

[14] S. G. Nikolov, E. Fernandez Canga, J. J. Lewis, A. Loza, D. R. Bull, and C. N. Canagarajah, "Adaptive Image Fusion Using Wavelets: Algorithms and System Design", in *Multisensor Data and Information Processing for Rapid and Robust Situation and Threat Assessment*, Eds. E. Lefebvre, P Valin, IOS Press, 2006.

[15] R.A. Mitchell and J.J. Westerkamp, "Robust Statistical feature based aircraft identification", *IEEE Trans. on Aerospace & Electronic Systems*, 35, 3, 1999.

[16] E. Blasch, J.J. Westerkamp, J.R. Layne, L. Hong, F. D. Garber and A. Shaw, "Identifying moving HRR signatures with an ATR Belief Filter," *SPIE* 2000.

[17] E. Blasch and M. Bryant, "SAR Information Exploitation Using an Information Filter Metric," *IEEE*, 1998.

[18] E. Blasch and S. Huang, "Multilevel Feature-based fuzzy fusion for target recognition," *Proc. SPIE* 2000.

[19] E. Blasch, and L. Hong, "Data Association through Fusion of Target Track and Identification Sets," *Fusion00*.

[20] W. Snyder, G. Ettinger and S. Laprise, "Modeling Performance and Image Collection Utility for Multiple Look ATR", *Proc. SPIE* 2003.

[21] K. Shaw and V. Bhatnagar, "Automatic Target Recognition using Eigen-Templates", *Proc. of SPIE*, Vol. 3370, 1998.

[22] B. V. K. Vijaya Kumar and M. Alkanhal, "Eigen-extended Maximum Average Correlation Height (EEMACH) Filters For Automatic Target Recognition", *Proc. SPIE*, Vol. 4379, 2001.

[23] F. Dicander and R. Jonsson, "Comparison of Some HRR-Classification Algorithms", *Proc. SPIE*, Vol. 4382, 2001.

[24] K. Ohba and K. Ikeuchi, "Recognition of Multi-Specularity Objects Using The Eigen-Window", *IEEE 1996 Proceedings of the 13th International Conf. on Pattern Recognition*, pp.692-696, 1996.

[25] L. M. Novak and G. J. Owirka, "Radar Target Identification Using An Eigen-Image Approach", *IEEE Radar Conference*, 1994.

[26] L.M. Novak, G.J. Owirka, A.L. Weaver, "Automatic Target Recognition Using Enhanced Resolution SAR Data", *IEEE Trans. On Aerospace & Elect. Sys.* Vol. 35, No. 1, January 1999.

[27] L. A. Chan, N. M. Nasrabadi, and D. Torrieri, "Discriminative Eigen Targets For Automatic Target Recognition", *Proc. of SPIE*, Vol. 3371, 1998.

[28] L. A. Chan, N. M. Nasrabadi, and D. Torrieri, "Eigenspace Transformation for automatic clutter rejection", *Optical Engineering*, Vol. 40 (4), 2001.

[29] V. Bhatnagar, A. K. Shaw, R. W. Williams, "Improved Automatic Target Recognition Using Singular Value Decomposition", *Proc. 1998 IEEE Conf. on Aco., Speech, & Sig. Proc.* Vol. 5, 1998.

[30] K. Shaw, R. Vashist, and R. Williams, "HRR-ATR using Eigen-Template with Noisy Observations in Unknown Target Scenario", *Proc. of SPIE*, Vol. 4053, 2000.

[31] S. Paul and A. K. Shaw, "Robust HRR Radar Target Identification By Hybridization Of HMM and Eigen-Template-Based Matched Filtering", *Proc of SPIE*, Vol. 5094, 2003.

[32] B. Kahler, J. Querns, G. Arnold, "An ATR Challenge Problem Using HRR Data'', *Proc. SPIE*, Vol. 6970, 2008.

[33] D. Gross, M. Oppenheimer, B. Kahler, B. Keaffaber, and R. Williams, "Preliminary Comparison of HRR Signatures of Moving and Stationary Ground Vehicles", *Proc. SPIE*, Vol. 4727, 2002.

[34] H-C. Chiang, R.L. Moses, and L.C Potter, "Model based classification of radar images", *IEEE Transactions on Information Theory*, 46, 5 (2000), 1842-1854.

[35] E.R. Keydel, S.W. Lee, J.T. Moore, "MSTAR Extended Operating Conditions: A Tutorial", *Proc. SPIE*, Vol. 2757, April 1997.

[36] J.C. Mossing, T.D. Ross, "An Evaluation Of SAR ATR Algorithm Performance Sensitivity To MSTAR Extended Operating Conditions", *Proc. SPIE*, Vol. 3370, April 1998.

[37] R. Williams, J. Westerkamp, D. Gross, and A. Palomino, "Automatic Target Recognition of Time Critical Moving Targets Using 1D High Range Resolution (HRR) Radar", *IEEE AES Systems Magazine*, April 2000.

[38] R. Wu, Q. Gao, J. Liu, and H. Gu, "ATR Scheme Based On 1-D HRR Profiles", *Electronic Letters*, Vol. 38, Issue 24, Nov. 2002.

[39] S. Paul, A. K. Shaw, K. Das, and A. K. Mitra, "Improved HRR-ATR Using Hybridization Of HMM and Eigen-Template-Matched Filtering", *IEEE Conf. on Aco., Speech, and Sig. Proc.*, 2003.

[40] W. Streilein, A. Waxman, *et al*, "Fused multi-sensor image mining for feature foundation data," *Fusion00*.

[41] K. Erickson and T. Ross, "Testbed for Architecture and Fidelity Trade Studies in the Bayesian Decision-Level Fusion of ATR Products," *Proc. SPIE*, Vol . 6567, 2007.

[42] J. D. Thompson, *Verification of a Decision Level Fusion Algorithm Using a Proven ATR System And Measured SAR Data*, M.S. Thesis, Air Force Institute Of Technology, 2006.